THE JOURNAL OF BIOLOGICAL CHEMISTRY VOL. 284, NO. 41, pp. 27875–27883, October 9, 2009

Multiple Rieske Proteins Enable Short- and Long-term Light Adaptation of *Synechocystis* sp. PCC 6803*

Received for publication, April 21, 2009, and in revised form, August 12, 2009 Published, JBC Papers in Press, August 12, 2009, DOI 10.1074/jbc.M109.011189

Yuichi Tsunoyama[‡§1], **Gábor Bernát**[‡1], **Nina G. Dyczmons**[‡], **Dirk Schneider**[¶], **and Matthias Rögner**[‡2]

From the [‡]*Department of Plant Biochemistry, Ruhr-University Bochum, 44780 Bochum, Germany, the* [§]*Division of Biology, Radioisotope Research Center, Kyoto University, Sakyo-ku, Kyoto 606-8502, Japan, and the* [¶]*Department of Biochemistry and Molecular Biology, ZBMZ, Albert-Ludwigs-University Freiburg, 79104 Freiburg, Germany*

In contrast to eukaryotes, most cyanobacteria contain several isoforms of the Rieske iron-sulfur protein, PetC, resulting in heterogeneity in the composition of the cytochrome b_6f complexes. Of three isoforms in the mesophilic cyanobacterium *Synechocystis* PCC 6803, PetC1 is the major Rieske protein in the cytochrome b_6f complex, whereas the physiological function of PetC2 and PetC3 is still uncertain. Comparison of wild type and various *petC*-deficient strains under selected light conditions revealed distinct functional differences: high-light exposure of wild type cells resulted in a significantly enhanced *petC2* transcript level, whereas a Δ*petC1* mutant showed a low cytochrome b_6f content, low electron flux, and a considerably increased accumulation of cytochrome-*bd* oxidase. In contrast to wild type and Δ*petC1*, Δ*petC2* and Δ*petC3* strains still grew fast under high-light conditions although all three Rieske proteins are required for maximal electron transport rates. Although the presence of PetC3 appears to be required for activation of the cyclic electron transport, state transitions were more effective in the absence of PetC2 and/or PetC3. In summary, our data suggest defined roles of the various PetC proteins in short- and long-term light adaptation.

In cyanobacteria the cytochrome b_6f complex is a shared component of the linear electron transport from water to $NADP^+$, of all types of cyclic electron transfer around photosystem 1 (PS1),[3] and of most types of pseudocyclic electron flows from water to the molecular oxygen (1–3). Therefore, this complex has a central and essential role in the complex cyanobacterial electron transport network (2). In general, the cytochrome b_6f complex catalyzes plastoquinol (PQH_2) oxidation and plastocyanin/cytochrome c_6 reduction and translocates protons across the thylakoid membrane (for recent reviews see Refs. 4–8).

Although linear photosynthetic electron transport from PS2 via cytochrome b_6f to PS1 results in both NADPH production and generation of a proton gradient (ΔpH) across the thylakoid membranes, cyclic electron flow(s) around PS1 establish(es) only a ΔpH, which is subsequently used for ATP generation. Thus, depending on the environmental (stress) and/or physiological conditions, the ATP:NADPH ratio can be adjusted to the required levels by tuning the cyclic-to-linear electron transport ratio. Beyond this, a redox poise of the PQ-pool via the cyclic/linear electron transport ratio adjustment is essential for both maximal light energy utilization and protection against photodamage or other types of stress (9–14). The dominant short-term (minutes) light-adaptation process in chloroplasts and cyanobacteria, by which the distribution of excitation energy transfer between the two photosystems is controlled, are the so-called state transitions (15, 16). By definition, in state I and state II the photosynthetic apparatus gives an optimal quantum yield of photosynthesis in light having a composition favoring its absorption by PS1 or PS2, respectively (17, 18). In the green alga *Chlamydomonas reinhardtii* state transitions are associated with a switching mechanism between linear and cyclic electron flow. Although state I, the light harvesting complex II (LHCII) is associated mainly with PS2 and is dominated by linear electron transport, state II with PS1-associated LHCII is governed by the cyclic one (18–20). In chloroplasts, state I to state II transition correlates with the activation of a kinase, which phosphorylates the LHCII leading to its lateral redistribution in favor of PS1. This activation is initiated by PQ-pool reduction and PQH_2 binding to the Q_o site of the cytochrome b_6f complex (21–23), which is suggested to result in a conformational change of the Rieske protein, a cytochrome b_6f core subunit, and finally leading to kinase activation (18, 23–25). Despite analogies to higher plants, the exact mechanism of state transitions in cyanobacteria is still under debate (for reviews, see Refs. 26 and 27). One major difference between chloroplasts and cyanobacteria is that instead of the membrane integral LHCII, the soluble light-harvesting phycobilisomes (PBS) capture light in cyanobacteria. They are located on the cytoplasmic surface of thylakoid membranes (28, 29) and transfer energy directly to the photosystems (30). Different from higher plants and green algae, cyanobacteria are in state I upon illumination and in state II in the dark or in very low light due to the respi-

* This work was supported by German Research Foundation Deutsche Forschungsgemeinschaft Grant SFB 480, project C1 (to M. R.) and SCHN 690/3-1 (to D. S.), grants from the Federal Ministry of Education and Research (BMBF) project Bio-H2 (to G. B.), the Kyoto University Foundation (to Y. T.), and the EU/NEST project Solar-H (to M. R.).

Dedicated to Prof. Dr. Mult. Achim Trebst on the occasion of his 80th birthday.

[1] Both authors contributed equally to this work.

[2] To whom correspondence should be addressed. Tel.: 49-234-3223634; Fax: 49-234-3214322; E-mail: Matthias.Roegner@rub.de.

[3] The abbreviations used are: PS1 and PS2, photosystem 1 and 2, respectively; C_t, threshold cycle numbers; CydA, cytochrome-*bd* oxidase subunit I; DCMU, 3-(3′,4′-dichlorophenyl)-1,1-dimethylurea; Fm^I and Fm^{II}, maximal chlorophyll fluorescence yield in states I and II, respectively; HL and LL, high- and low-light, respectively; MV, methyl viologen; P_{700}, the primary electron donor of PS1; PBS, phycobilisome; PC, phycocyanin; PetC, Rieske iron-sulfur protein of cytochrome b_6f; PQ and PQH_2, plastoquinone and plastoquinol, respectively; SU IV, subunit IV of cytochrome b_6f; WT, wild type; LHCII, light harvesting complex II; qPCR, quantitative PCR; APC, allophycocyanin; FR, far red.

ratory electron flow reducing the PQ-pool (31, 32). According to available data, in cyanobacteria both the relative energy transfer from phycobilisomes to photosystems and the distribution of the absorbed light energy are regulated by state transitions, although the components of the regulatory signal cascade are essentially not known (26). Although no Rieske protein-mediated kinase activation has been described in cyanobacteria, it is assumed that the triggering mechanism is similar in cyanobacteria (26). Thus, besides its above described central function in electron transport and energy transduction processes, the cytochrome b_6f complex can also be involved in regulating excitation energy distribution between PS1 and PS2 (4, 18, 20–26), as well as in an assembly mediated control of protein synthesis (25). Experimental data indicate that the Rieske iron-sulfur protein plays a key role in both processes.

Rieske iron-sulfur proteins are essential functional subunits of the cytochrome b_6f complex. The Rieske protein binds a redox-active [2Fe-2S] center close to the *p*-side of the membranes and carries electrons in the high-potential branch of the bifurcated electron transport chain of the complex (4, 5, 7, 8). The cytochrome b_6f monomer consist of four large (17.5–32 kDa) core subunits, cytochrome *f* (PetA), cytochrome b_6 (PetB), the Rieske iron-sulfur protein (PetC), and subunit IV (SU IV, PetD), as well as four additional small (3.3–4.1 kDa) subunits, PetG, PetL, PetM, and PetN (7, 33). Except for PetL and PetM all subunits are required for a functional cytochrome b_6f complex (34, 35). Besides these *bona fide* subunits additional weakly associated subunits are also reported (36, 37). The PetC (Rieske) protein has a single N-terminal located transmembrane helix followed by a mobile, water-soluble domain with the [2Fe-2S] cofactor binding regions, which extends into the thylakoid lumen. The α-helix and the soluble domain are connected by a flexible "hinge" region.

In the genome of eukaryotes and in some cyanobacteria the cytochrome b_6f complex Rieske protein is encoded by a single *petC* gene. In contrast, in most cyanobacteria several Rieske isoforms exist, which are encoded by a *petC* gene family (for a review, see Ref. 38). The *Synechocystis* PCC 6803 genome contains three *petC* genes, *petC1* (*sll1316*), *petC2* (*slr1185*), and *petC3* (*sll1182*) (39), which encode corresponding Rieske proteins PetC1, PetC2, and PetC3, respectively. Although PetC1 and PetC2 show high sequence identity, PetC3 differs significantly. *In vivo* analysis of *petC* gene-deficient mutant strains have indicated that PetC1 is the major Rieske iron-sulfur protein in *Synechocystis* PCC 6803 (40). Moreover, PetC3 has a much lower midpoint potential (+135 mV) than PetC1 and PetC2 (300–320 mV), suggesting that different electron donors have to reduce PetC3 (41). In *Nostoc* sp. PCC 7120, the PetC4 protein, which has a high sequence similarity to PetC1 and PetC2, has a role in nitrogen fixation and/or heterocyst formation and is also proposed to be a redox sensor (38). However, despite these suggestions, the physiological significance of *petC* multiplicity in cyanobacteria remains unclear.

In the present report we analyze low- and high-light-treated wild type (WT) and *petC*-deficient *Synechocystis* PCC 6803 strains on the transcript, the protein, and on a functional level to assign specific functions to the three different PetC proteins in light acclimation and electron transport processes. We observed alterations in cell growth of different Δ*petC* mutant strains under high-light conditions. Our experiments also revealed various effects of the individual Rieske proteins on photosynthetic electron transport and the distribution of excitation energy between the two photosystems. Furthermore, accumulation of *petC2* mRNA in WT cells as response to high light was shown by real time quantitative PCR (qPCR). Based on these results, we discuss the potential roles of the *Synechocystis* PetC1, PetC2, and PetC3 in regulation and light adaptation and propose a functional model with regulatory pathways.

EXPERIMENTAL PROCEDURES

Growth Conditions—Construction of single and double *petC* deletion (Δ*petC*) strains from *Synechocystis* PCC 6803 is described in detail in Ref. 40. *Synechocystis* WT and mutant strains were grown in BG-11 medium (42) at 30 °C in glass tubes bubbled with 5% CO_2-enriched air. Liquid medium for culturing Δ*petC1*, Δ*petC2*, and Δ*petC3* strains as well as agar plates were supplemented with 30 μg/ml of chloramphenicol, 100 μg/ml of spectinomycin, or 50 μg/ml of kanamycin, respectively. The culture medium for double mutants contained both corresponding antibiotics. Low-light (LL, 40 μmol photons m^{-2} s^{-1}) and medium to high-light (HL) illumination (100–650 μmol photons m^{-2} s^{-1}) were provided by white fluorescent and halogen lamps, respectively. Photon flux densities were determined with a QRT1 light meter (Hansatech).

Pigment Analysis—Pigment concentrations of the cultures are given per cell number with cell densities determined with a Z2 Coulter counter (Beckman Coulter, Fullerton, CA). Absorption spectra were recorded by a Hitachi U-3000 dual-beam spectrophotometer equipped with a 60-mm integrating sphere. Phycocyanin and chlorophyll concentrations were determined according to Ref. 43, and the phycocyanin/allophycocyanin ratio as in Ref. 44.

RNA Preparation and Quantitative PCR—10-ml cultures of WT cells were harvested at A_{730} = 0.2 by centrifugation (6000 × *g*, 4 °C, 10 min), suspended in 1 ml of diluted 1:4 RNA Protect Bacteria Reagent (Qiagen) in Tris-EDTA buffer (TE), and subsequently incubated on ice. Upon washing with TE buffer cells were suspended in 1 ml of saturated sodium iodide solution and subsequently washed twice with TE buffer. The cells were disrupted with glass beads in 350 μl of RNeasy lysis buffer (Qiagen) using a Mini-Beadbeater (Biospec). Isolation of total RNA was accomplished using the RNeasy mini kit (Qiagen) according to the manufacturer's instructions. The obtained RNA was treated with 2 units of TURBO DNase (Ambion) for 20 min at 37 °C to remove DNA contamination, and the reaction was subsequently terminated by addition of the DNase inactivation reagent (Ambion). 1 μg of purified RNA was used for cDNA synthesis using a Quantitect reverse transcription kit (Qiagen) according to the manufacturer's instructions.

cDNA synthesis was followed by real time qPCR in a DNA Engine Opticon 2 Real-time PCR Detection System (Bio-Rad), using 20 μl of reaction mixture supplied by the qPCR Core kit for SYBR® Green I (Eurogentec) containing 250 nM primers. The following primers were used for amplification: petC1F (5′-CCAGTACAACGCTGAAGGT-3′) and petC1R (5′-CCAGG-

TGCTGAGCACTAAT-3′) for *petC1*; petC2Fneu2 (5′-CCGTCGTCAATTACTCAACT-3′) and petC2Rneu2 (5′-TTGGCAATAATGCCTCCTC-3′) for *petC2*; petC3F (5′-AGTAACGGCCAAGGACAA-3′) and petC3R (5′-CGCACTAATCTGGCCACTA-3′) for *petC3*; rnpBF (5′-GAGAGTTAGGGAGGGAGTTG-3′) and rnpBR (5′-GTCAGTTACCAGTTAGTCAGC-3′) for *rnpB*. 40 cycles with a 15-s incubation at 95 °C and a 1-min incubation at 60 °C were applied. Changes in the mRNA levels were determined by relative quantification (45, 46). Threshold cycle numbers (C_t), real time PCR efficiency (E), and relative expression ratios were calculated using Opticon Monitor 2.02, LinRegPCR (47), and the Relative Expression Software Tool (REST®) (48), respectively.

SDS-PAGE and Western Blot Analysis—45 ml of WT and Δ*petC* cells were harvested at $A_{730} = 0.2$ and dispersed in 75 μl of SDS-PAGE loading buffer. Cells were broken by vortexing with glass beads and a subsequent 15-min sonication (Brandelin Sonorex, Berlin, Germany) at 4 °C, followed by a 5-min incubation at 95 °C. After centrifugation, the supernatant was collected and stored at −20 °C until use. 5 μl of supernatant was separated by SDS-PAGE on a 12% SDS gel (49) and blotted on a polyvinylidene difluoride membrane. PetC1/2/3, cytochrome *f*, cytochrome b_6, SU IV, as well as the CydA subunit of the cytochrome-*bd* oxidase were detected by immunoblotting using polyclonal antibodies (37, 41). The PetC2 and CydA antibodies was raised against synthesized peptide fragments DQIFISPWTDLDPRTGEKP (Iwaki, Tokyo, Japan) and KLAAMEALWETVPA (Davids Biotechnologie, Regensburg, Germany), respectively. The rabbit primary antibodies and the goat anti-rabbit IgG alkaline phosphatase-conjugated secondary antibody (Sigma) were used at dilutions of 1:2500 and 1:25000, respectively. Membranes were incubated with nitro blue tetrazolium chloride and 5-bromo-4-chloro-3′-indolyl phosphatase *p*-toluidine salt (Roche) at room temperature to visualize cross-reacting protein bands. Band intensities for protein quantification were established using ImageJ.

Measurement of State Transitions—State transitions in WT and mutant cells were monitored by two distinct methods. Although low temperature fluorescence emission spectra were recorded after PBS excitation as described previously (37), chlorophyll fluorescence transients at room temperature were measured in a Dual-PAM-100 measuring system (Heinz Walz GmbH) by adapting the method of Kovács and co-workers (50) to cyanobacteria. State I to state II and state II to state I transitions were induced by switching off and on PS1 light, respectively. PS1 was selectively excited by far red (FR) light using 730 nm LEDs of the DUAL-E measuring head set to their maximal light intensity (~40 relative units). 300-ms saturating pulses (I = 10000 μmol photons m^{-2} s^{-1}) were applied in state I and state II to probe the Fm^I and Fm^{II} fluorescence levels, respectively.

P_{700}^+ Reduction Kinetics and Quantification of the Linear and Cyclic Electron Transport Rates—P_{700}^+ reduction kinetic decays in LL- and HL-adapted cells were recorded with a dual PAM-100 measuring system at a chlorophyll concentration of 5 μg/ml as described in Ref. 51. Complete P_{700} oxidation was achieved by 100-ms saturating pulses (I = 10000 μmol photons m^{-2} s^{-1}). Averages of three individual traces were taken. Rate constants (k) in the absence or presence of linear and/or (direct) cyclic electron transport inhibitors, 3-(3′,4′-dichlorophenyl)-1,1-dimethylurea (DCMU) and methyl viologen (MV), respectively, were determined by fitting the decays by single exponential functions. The linear and cyclic electron transport activities were quantified as the differences of certain rate constant combinations. Although the rate constant of the linear electron transport was considered to be the mathematical difference of the rate constants determined in non-treated and DCMU-treated samples, the direct cyclic electron transport was calculated as difference of the corresponding k values of non-treated and MV-treated samples. Note that the direct cyclic electron transport may consist of several parallel individual routes (3), which were not distinguished.

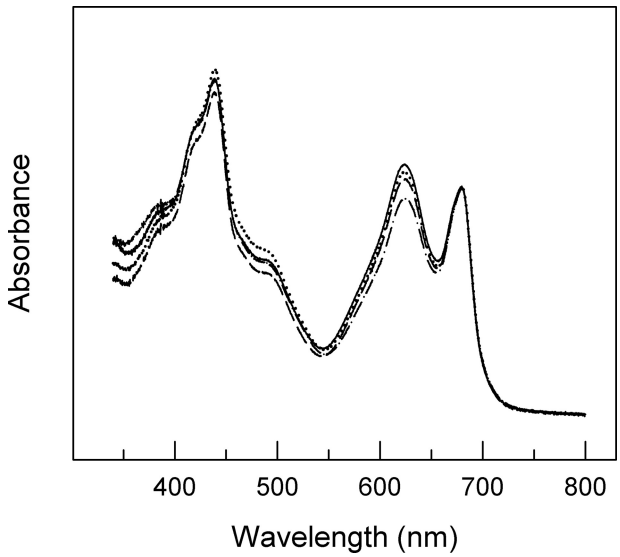

FIGURE 1. **Absorption spectra of WT (*solid line*) and *petC*-deficient *Synechocystis* PCC 6803 strains (Δ*petC1*, *dashed*; Δ*petC2*, *dash-dotted*; Δ*petC3*, *dotted*).** Spectra are normalized to the absorption peak at 679 nm.

RESULTS

Pigment and Protein Composition—Up to now the physiological function of *petC* heterogeneity in cyanobacteria is essentially not understood. Usually, the construction of knock-out strains is a highly valuable standard method to elucidate the potential *in vivo* function of such proteins. The generation of Δ*petC Synechocystis* strains has been reported recently (40), and it has already been shown that electron transfer is modified at least in the Δ*petC1* strain and that PetC2 can partly replace the major Rieske protein PetC1. However, it is unknown whether the absence of PetC1 (or the other PetC isoforms) influences pigment compositions in the cells or affects the expression, accumulation, or stability of the cytochrome b_6f complex. To test these issues, we analyzed the chlorophyll, phycocyanin (PC), and allophycocyanin (APC) contents as well as the accumulation of the four large cytochrome b_6f complex core subunits (including all three PetC isoforms) in WT and various Δ*petC* strains (Figs. 1 and 2*A*). Absorption spectra of WT and the three *petC* single deletion mutants are shown in Fig. 1. All strains have the typical major chlorophyll absorption peaks at 439 and 679 nm and a PBS absorption peak at 625 nm. The PC/chlorophyll ratio is very similar in WT, Δ*petC1*, and

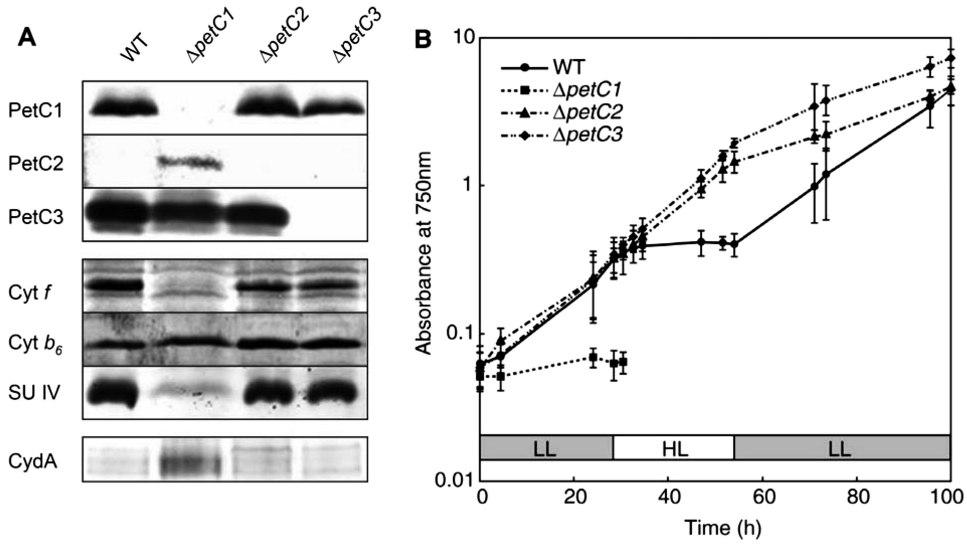

FIGURE 2. *A*, immunological analysis of WT and *petC*-deficient *Synechocystis* PCC 6803 strains using antibodies against the major subunits of the cytochrome b_6f complex (cytochrome *f*, cytochrome b_6, and SU IV) and CydA. *B*, effects of HL on growth rates of WT and Δ*petC* mutants. Cultures with identical initial optical densities have been exposed to LL for 28 h, followed by HL illumination for 30 h, and then by LL again. *Error bars* indicate the S.D. of three to five independent experiments.

TABLE 1

Pigment composition of *Synechocystis* PCC 6803 WT and *petC* single deletion strains

Cells were grown under LL. Data are expressed as mean ± S.D. ($n = 3$). Determination of the various parameters and ratios is described under "Experimental Procedures."

Strain	Chlorophyll/10 cells	PC/10 cells	PC/chlorophyll	PC/APC
	μg	μg	μg	μg
WT	3.8 ± 0.5	25 ± 4	6.6 ± 0.3	3.6
Δ*petC*1	4.5 ± 0.8	26 ± 7	5.6 ± 0.6	1.4
Δ*petC*2	4.0 ± 1.3	20 ± 8	4.8 ± 0.5	3.4
Δ*petC*3	7.4 ± 1.4	46 ± 10	6.2 ± 0.3	3.0

Δ*petC3* strains (Table 1), whereas it is significantly lowered in the Δ*petC2* strain. Noteworthy, by light microscopy we observed that the Δ*petC3* cells are considerably bigger (3.4 *versus* 2.7 μm) when compared with the WT or to the other deletion strains. This increased cell size results in increased chlorophyll and PC content per cell (Table 1), although the PC/chlorophyll ratio is similar to that for WT cells. Furthermore, the ratio of PC to APC is about the same in all but the Δ*petC1* strain (Table 1). This indicates an unchanged protein composition of the light harvesting PBSs in the absence of *petC2* or *petC3* genes and a decrease in size of the PBS rod complexes upon *petC1* deletion.

Expression of the individual PetC isoforms in the various strains as well as expression of the other three cytochrome b_6f complex core subunits was tested by immunoblot analysis (Fig. 2*A*). Although all three PetC isoforms are expressed in the WT strain (see below), only PetC1 and PetC3 were detected by immunoblot analysis. The cellular content of PetC1 and PetC3 is similar in the WT and mutant strains where the corresponding genes are not deleted (Fig. 2*A*). Because the amount of the other three large cytochrome b_6f subunits in Δ*petC2* and Δ*petC3* strains were similar to WT cells (Fig. 2*A*) a comparable cytochrome b_6f complex population size can be assumed in these mutant strains. However, the protein profile in the Δ*petC1* strain is quite different when compared with WT cells and other mutant strains. First, expression of the PetC2 protein was only detected in this strain by immunoblot analysis. Second, this mutant also showed a drastic decrease of accumulated cytochrome *f* and SU IV (Fig. 2*A*) indicating a defect in formation of functional cytochrome b_6f complexes upon deletion of *petC1*. As an increase in the cytochrome-*bd* oxidase activity in the Δ*petC1* strain had already been observed (35, 40), we also tested the expression of the major cytochrome-*bd* oxidase subunit I (CydA) both in WT and Δ*petC* strains (Fig. 2*A*): whereas CydA was essentially undetectable by immunoblot analysis in WT, Δ*petC2*, and Δ*petC3* strains, its expression was dramatically increased in the Δ*petC1* strain. This is in good agreement with earlier observations of a significantly increased cytochrome-*bd* oxidase activity in the Δ*petC1* strain (40). Most likely, due to cytochrome b_6f complex deficiency in the Δ*petC1* strain, cytochrome-*bd* oxidase has to partly take over the role of the cytochrome b_6f complex in PQH_2 re-oxidation to keep electron transport and energy transduction efficient, *i.e.* to keep the cells alive.

Effect of Light Conditions on Growth Rates of WT and petC-deficient Synechocystis Strains—Although *Synechocystis* Δ*petC* single and double deletion strains have already been initially characterized (40), these results reflect only cells grown under LL growth conditions. To investigate the effect of light intensity, these mutant cells were grown under LL for 1 day followed by HL illumination for 30 h and a subsequent reset to the LL regime. In agreement with our previous results (40), WT, Δ*petC2*, and Δ*petC3* strains showed approximately the same growth rates, whereas the Δ*petC1* strain grew significantly slower under LL growth conditions. Upon switching from LL to HL, the Δ*petC1* cells died and the cultivation was discontinued (Fig. 2*B*). HL also had a severe impact on the viability of WT cells (Fig. 2*B*), slowing down its growth rate gradually to zero during the first 6 h of HL illumination. These cultures returned to normal growth under LL conditions. In contrast, Δ*petC2* and Δ*petC3* strains showed constant growth during the continuous 30-h HL, similar to the Δ*petC2*/*C3* double deletion strain (data not shown). A WT strain with an intact genome should typically not be less resistant against light stress than knock-out strains, these results could indicate that the *petC2* and *petC3* gene products are involved in regulatory processes, which might protect the organism against photo-damage.

High Light Induces an Elevated petC2 Gene Expression—To further elucidate the role of the various *petC* gene products in light acclimation we examined the effect of high light on the mRNA expression level of the three *petC* genes in *Synechocystis* PCC 6803 WT by qPCR. For these experiments, the expression of the *rnpB* gene, which is independent of light intensity (52),

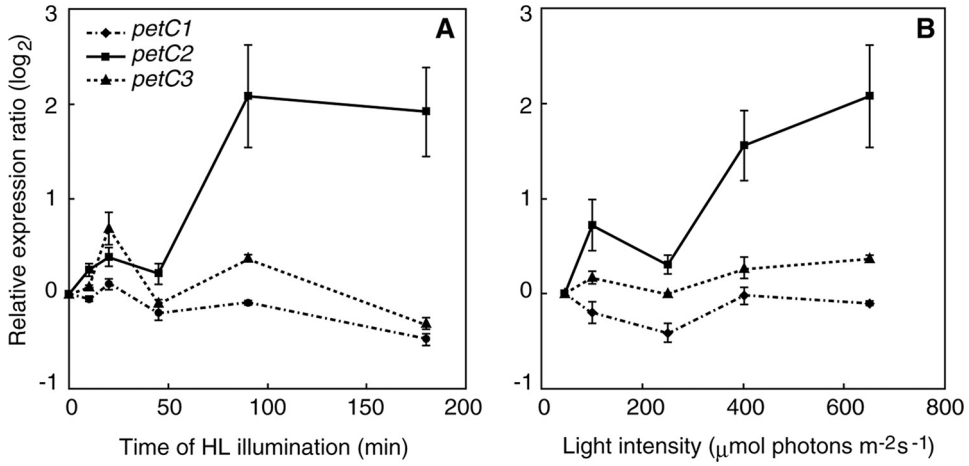

FIGURE 3. **Accumulation of *petC* transcripts in *Synechocystis* PCC 6803 WT cells as determined by qPCR analysis.** The *y* axis shows the relative expression ratio ($\log_2$ scale), calculated by REST (see "Experimental Procedures"), relative to cells grown under LL conditions. The *error bars* represent the S.D. of three to nine independent measurements. *A*, cells at $A_{750} = 0.2$ were incubated under HL for 10, 20, 45, 90, or 180 min. *B*, accumulation of *petC* transcripts after incubation of *Synechocystis* cells at various light intensities. Cells were incubated for 180 min at elevated light intensities (100, 250, 400, and 650 μmol photons m^{-2} s^{-1}).

was used as the internal control. In qPCR analysis, the threshold cycle number (C_t) is the fractional PCR cycle number, at which the emitted fluorescence exceeds the fixed threshold (background) fluorescence, *i.e.* a higher initial amount of a specific mRNA in a given sample results in an earlier detection in the PCR as fluorescence increase. Therefore, a lower C_t value reflects a higher expression of a certain gene. C_t values for the *petC1*, *petC2*, *petC3*, and *rnpB* genes in LL-adapted samples were 21.25 ± 0.90, 31.34 ± 1.85, 24.83 ± 1.01, and 17.12 ± 1.15, respectively, whereas the corresponding values in cells illuminated by HL for 90 min were 19.70 ± 0.74, 26.73 ± 0.87, 23.71 ± 0.64, and 16.12 ± 0.75, respectively ($n = 9$). Calculated PCR efficiencies (*E*) for *petC1*, *petC2*, *petC3*, and *rnpB* were 1.76, 1.52, 1.70, and 1.96, respectively. These results clearly show that under both LL and HL conditions the expression level of *petC2* was lower than *petC1* and *petC3* in *Synechocystis*, which was confirmed with different primer sets for the *petC2* transcript amplification (data not shown). This significant decrease of the *petC2* C_t value under HL conditions clearly indicates an induction of the *petC2* expression. The time course of *petC* transcript accumulation during HL is shown in Fig. 3*A*, whereas Fig. 3*B* shows the dependence of *petC* expression after a 90-min exposure to different light intensities. It is apparent from both panels that the expression levels of *petC1* and *petC3* are quite independent from the illumination time and light intensities, whereas *petC2* expression increases with both light intensity and time. A significant increase in the *petC2* transcript level was observed after a 90-min HL incubation (Fig. 3*A*) and above a light intensity of 350–400 μmol photons m^{-2} s^{-1} (Fig. 3*B*).

Linear and Cyclic Electron Transport Activities—The *petC2* transcript level is significantly enhanced in *Synechocystis* WT grown under HL conditions (Fig. 3), and growth of the Δ*petC2* and Δ*petC3* mutants was not suppressed by HL, in contrast to WT cells (Fig. 2*B*). To investigate the impact of *petC* deletions on electron transport activities under HL illumination, overall, linear and cyclic electron flow were quantified in LL- and HL-adapted *Synechocystis* cells using P_{700}^+ reduction kinetics. Fig. 4*A* illustrates the principles of this quantification: as an example, curves of WT *Synechocystis* cells adapted to LL conditions are shown. The time interval of the saturating pulse (100 ms, indicated as *black rectangle* over the traces) is followed by the (dark) reduction of P_{700}^+, which shows the fastest kinetics in untreated cells (*curve 1*). Addition of MV (*curve 2*), which blocks cyclic electron transport, DCMU (*curve 3*), which blocks linear electron transport, or a combination of them (*curve 4*), slowed down the reduction kinetics. The corresponding rate constants for linear and cyclic electron transport were determined as the difference of the two rate constants obtained by fitting the decays with single exponential functions in an appropriate combination (for details see "Experimental Procedures"). Fig. 4*B* summarizes the determined rates for *Synechocystis* WT and the various Δ*petC* strains under LL and HL conditions and in Fig. 4*C* the relative contribution of linear and cyclic electron transport activities are shown. Although linear electron transport is the dominant form in all photoautotrophic cultures (Fig. 4*B*, *white columns*) both electron transport activities and their response to HL showed large variations between individual strains. First of all, the highest overall and linear electron transport activity was detected in WT cells with all three PetC proteins expressed. This indicates that all PetC isoforms are needed for maintaining maximal electron transport rate. Electron transport activities of LL cultures were considerably lower in the absence of PetC2 and/or PetC3. The observed very low electron transport activity in the Δ*petC1* strain (and also in the Δ*petC1/3* strain, data not shown) was most likely caused by the rather low population size of active cytochrome b_6f complexes upon deletion of *petC1* (compare Fig. 2*A*). Although in WT and Δ*petC2* strains the overall and linear electron transport rates are reduced under HL conditions in comparison to LL conditions, changes in Δ*petC1* and Δ*petC3* strains are within the range of error (Fig. 4*B*). In all strains an up-regulation of the cyclic electron transport was observed under HL conditions (Fig. 4*C*). Notably, the relative contribution of the cyclic electron transport was significantly higher in the two strains containing PetC3 (Δ*petC1* (26%) and Δ*petC2* (27%)) than in the Δ*petC3* deletion strains (14%) and WT cells (9%) (Fig. 4*C*).

Energy Transfer and Short-term Light Adaptation (State Transitions)—Upon excitation at 580 nm, low temperature (77 K) fluorescence emission spectra enable tracking of energy transfer from PBS antenna to photosystems in cyanobacteria. Although peaks at 685/695 and 725 nm (Fig. 5*A*) indicate energy transfer from PBS to PS2 and PS1, respectively, emission peak and the shoulder at 650 and 665 nm indicate functionally unconnected PC and APC, respectively. The relatively high PBS to PS1 energy transfer (Fig. 5*A*, *solid line*) confirms that dark adaptation induces state II in *Synechocystis* WT. In contrast,

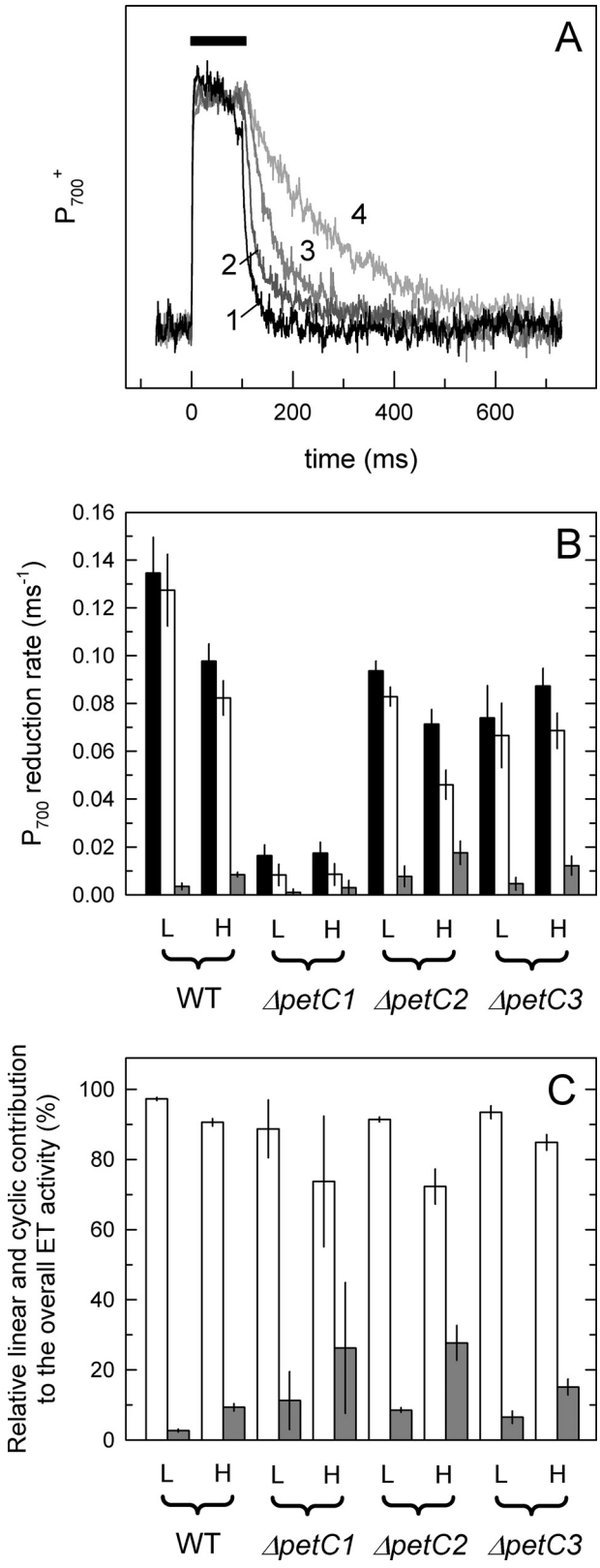

FIGURE 4. **Quantification of linear and cyclic electron transport by P_{700} redox kinetic measurements.** *A*, kinetic traces of LL-adapted WT cells. The *black rectangle* symbolizes the time interval of the saturating light pulse (100 ms), which is followed by the reduction of P_{700}^{+} (in the dark). The fastest kinetics observed in the untreated sample (*curve 1*), which is slowed down in the presence of MV (*curve 2*) and/or DCMU (*curves 3* and *4*) due to blocked cyclic and/or linear route(s), respectively. Curves correspond to three averaged traces of the same sample. Rate constants were determined by fitting the curves with single exponential functions. Individual rate constants of linear and cyclic electron transfer (*B*) were determined as described under "Experimental Procedures" and in Ref. 51, and for comparison normalized to the overall electron transport activities (*C*). *Black*, *white*, and *gray columns* represent the determined overall, linear, and cyclic activities, respectively. Electron transport rates are averaged from measurements with three to five independent cultures. Activities of HL samples have been determined after 180 min of HL illumination.

selective illumination of PS1 with far-red light oxidizes the PQ pool and induces state I with increased energy transfer from PBS to PS2 (Fig. 5*A*, *dashed line*). Comparison of WT with various *petC* mutants (Fig. 5, *A–D*) shows major differences in the capability of *Synechocystis* to perform state transitions: different from Δ*petC2* and Δ*petC3* strains (Fig. 5, *C* and *D*, respectively), Δ*petC1* cells seem to have essentially lost the capability for state transitions (Fig. 5*B*). Also, the "state transition efficiency" was higher in the Δ*petC2* and Δ*petC3* mutants than in WT (with the positions of PBS and photosystem emission peaks being identical). The spectral characteristics of double deletion strains Δ*petC1/3* and Δ*petC2/3* were similar to single deletion mutants Δ*petC1* and Δ*petC2* or Δ*petC3*, respectively (data not shown). The high APC/PC ratio in the Δ*petC1* mutant deduced from absorption measurements (Table 1) was also seen in the fluorescence spectra of this strain (*i.e.* higher ratio of the fluorescence emission at 665 and 650 nm; Fig. 5*B*).

In addition to low temperature fluorescence emission spectra, state transitions can also be followed by room temperature chlorophyll fluorescence transients. According to the method of Ruban and co-workers (50), state transitions can be induced by switching on and off PS1 light in the presence of continuously applied PS2 light. Also, maximal fluorescence levels that should be different in states I and II (denoted as Fm^{I} and Fm^{II}, respectively) can be probed by saturating light pulses (50). Although the transients upon PS1-light on/off reflect the capacity of state transitions to balance the PQ redox state, Fm^{I}–Fm^{II} oscillations provide information on changes in the apparent (PS2) antenna cross-section.[4] Fig. 5, *E–H*, show the results upon adaptation of this method for cyanobacteria. As in contrast to chloroplasts the cyanobacterial PQ-pool was significantly reduced in the dark (due to respiratory electron transfer), a pre-reduction of the PQ-pool by PS2 light was not required. PS1 light (Fig. 5*E*, *left arrow*) induces a gradual increase of chlorophyll fluorescence, reflecting an increasing PS2 antenna cross-section during state II to state I transition. Light off (*downward arrow*) causes a rapid transient rise that was followed by decay to the original dark level. This indicates a temporary increase in the PQ reduction level (absence of PS1 oxidation power), which was followed by PQ re-oxidation and a decrease of PS2 antenna cross-section (state I to II transition). Changes in the apparent antenna cross-section can be visualized by saturating light pulses after dark and FR periods, revealing Fm^{II} and Fm^{I}, respectively. Results presented in Fig. 5, *F–H*, agree well with low temperature fluorescence spectra (Fig. 5, *B–D*) in showing big differences in the *petC*-mutants to perform state transitions. In contrast to Δ*petC2* and Δ*petC3* strains (Fig. 5, *G* and *H*, in comparison with *C* and *D*, respectively),

[4] A. V. Ruban, personal communication.

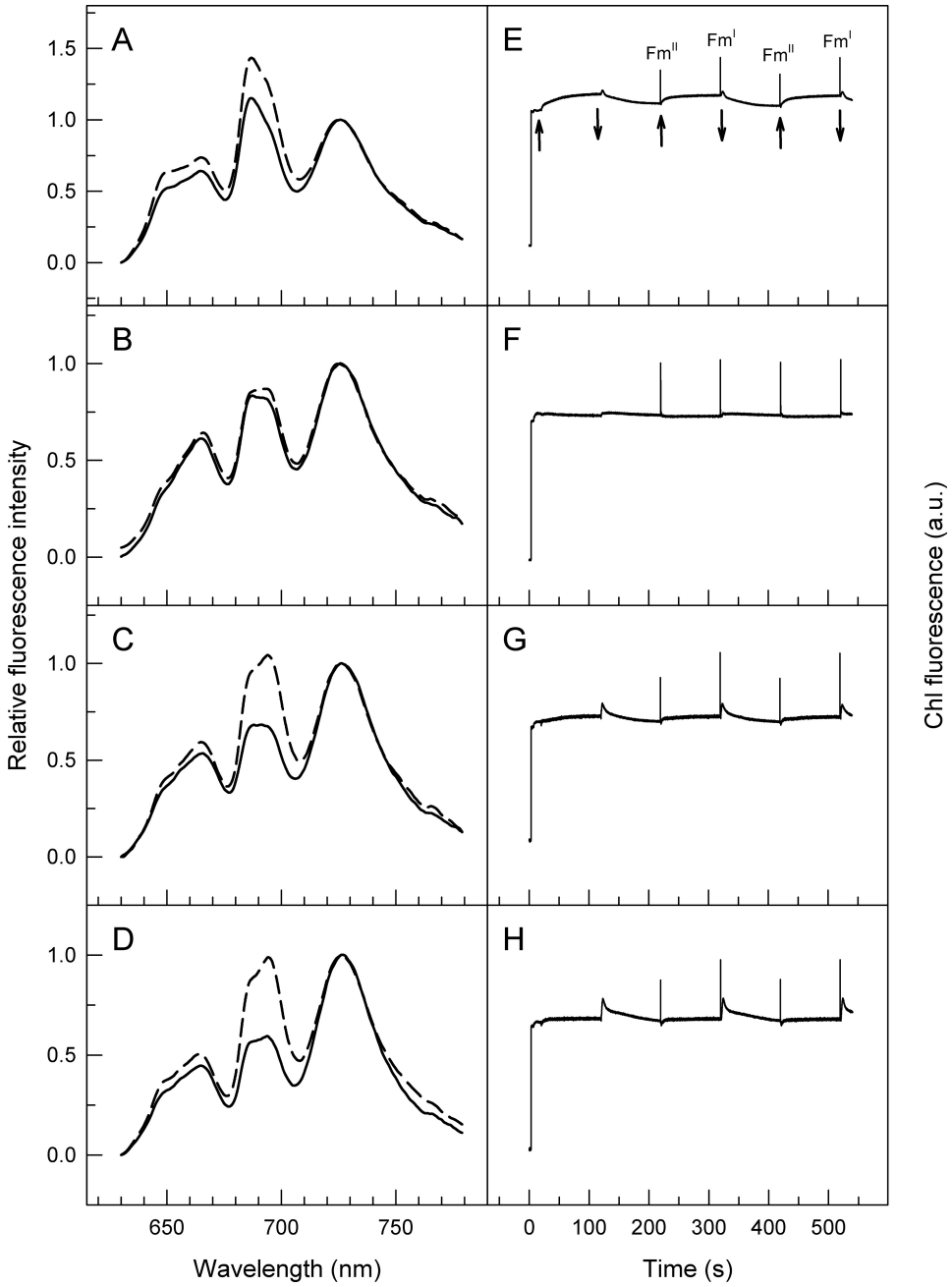

FIGURE 5. **State transitions followed by low temperature (77 K) fluorescence spectroscopy (*A–D*) or room temperature chlorophyll fluorescence (*E* – *F*) in WT (*A* and *E*), Δ*petC1* (*B* and *F*), Δ*petC2* (*C* and *G*), and Δ*petC3* (*D* and *H*) cells of *Synechocystis* PCC 6803.** *Left panels*, excitation wavelength of 580 nm; *solid* and *dashed curves* represent two parallel samples that have been frozen after a 15-min dark incubation or after a subsequent FR illumination, respectively. All curves were normalized to the emission peak at 725 nm. *Right panels*, *upward* and *downward arrows* indicate "on" and "off" of FR illumination, respectively. Saturation pulses were given to record Fm in states I and II.

were more pronounced in Δ*petC2* and Δ*petC3* mutants than in WT (Fig. 5, *G* and *H*). This indicates significant transient changes in the PQ redox level that in turn induce a more robust change in the PS2 antenna cross-section. These dynamic changes in distribution of absorbed light energy between the two photosystems during state transitions can be followed by fluorescence measurements both at low (*left panels*) and at room temperature (*right panels*).

DISCUSSION

PetC1 Is the Major Rieske Protein—Although in higher plants and green algae the Rieske [2Fe-2S] protein of the cytochrome b_6f complex is encoded by a single *petC* gene, in *Synechocystis* PCC 6803 and other cyanobacteria three (or even more) different *petC* genes code for a group of putative Rieske isoforms. On the phylogenetic tree of Rieske iron-sulfur proteins, only PetC1 of *Synechocystis* forms a branch with other cyanobacteria containing merely one *petC* gene, and this branch is phylogenetically close to the group of chloroplast Rieske proteins (38, 41). Based on an initial characterization of *Synechocystis* Δ*petC* strains it has already been suggested that PetC1 is the major Rieske iron-sulfur protein in *Synechocystis* (40). Deletion of *petC1* results in a highly reduced PQ-pool when respiratory electron transport is inhibited as well as in an increased PS1 to PS2 ratio (40), although this ratio was not altered in the Δ*petC2* or Δ*petC3* strains (40). In line with this, deletion of *petC1* also results in diminished PS2 activity (40). Our present work further refines this predominant and crucial role of PetC1 in electron transport of *Synechocystis*. As evident from Fig. 4*B* (linear and cyclic), electron flow via the cytochrome b_6f complex is severely affected in the Δ*petC1* strain, resulting in incomplete oxidation of the PQ-pool by PS1 (Fig. 5*F*) and in a light-sensitive growth phenotype (Fig. 2*B*). The diminished electron flux through the cytochrome b_6f complex and, as a consequence, the easy reduction of the PQ-pool also severely affects the *Synechocystis* growth rate even under low-light conditions (Fig. 2*B*).

Δ*petC1* cells have lost the capability to perform state transitions (Fig. 5*F*): neither significant transient changes in the steady-state fluorescence level nor changes in the antenna cross-section were induced by switching on or off FR illumination. In agreement with the results of P_{700}^+ reduction kinetic experiments (Fig. 4) this shows an impaired electron flow through the cytochrome b_6f complex, and in turn, a small impact of the PS1 on the plastoquinol oxidation. On the other hand, the Fm^I–Fm^{II} oscillation and fluorescence changes (with FR on and off)

Due to the diminished electron transport through the cytochrome b_6f complex, the PQ-pool appears never to be sufficiently oxidized by PS1 to induce a state transition in the Δ*petC1* strain, *i.e.* the cells remain in state II under all conditions (Fig. 5, *B* and *F*). A similar effect was recently reported for *Synechocystis* with the deleted *ssr2998* gene (37). In these mutants the limited capabilities to control the PQ redox level by state transitions is compensated by adjusting the PS2 to PS1 ratio (37, 40). The lowered PC/APC ratio in the Δ*petC1* strain (Table 1, Fig. 5*B*) also decreases electron input into the PQ-pool and may help in maintaining the redox state of the PQ pool.

Deletion of the *petC1* gene is apparently accompanied by increased *cydA* gene expression as shown by immunoblot analysis of CydA accumulation (Fig. 2*A*). Although an increased cytochrome-*bd* oxidase activity has already been suggested based on fluorescence induction measurements of mutants with impaired cytochrome b_6f complexes (35, 40), this is the first direct proof for the presence of the cytochrome-*bd* oxidase in a cyanobacterial thylakoid membrane on the protein level. (For the original paper on the cytochrome-*bd* oxidase as a component of the cyanobacterial electron transport network, see Ref. 53; for two recent ones, see Refs. 54 and 55.) Thus, reduction of the cytochrome b_6f complex activity and the resulting easily reducable PQ-pool do not only influence the regulation of the PS2 to PS1 and PC/APC stoichiometry but also seem to induce expression of cytochrome-*bd* oxidase.

Because the cytochrome b_6f complex is a central and essential component of the energy-transducing system in chloroplasts and cyanobacteria deletion of *petC* should not be possible if there is only a single *petC* gene in the genome. The green alga *C. reinhardtii* is the only known example for a viable Δ*petC* mutant (56), being able to grow heterotrophically and to generate ATP and NAD(P)H solely by oxidative phosphorylation in mitochondria. Even the cyanobacterium *Synechococcus* PCC 7002, with a genome containing three *petC* gene copies, was unable to survive *petC1* deletion (57). In contrast, in *Synechocystis* PCC 6803 *petC1* can be deleted and partially substituted by PetC2 (40), and deletion of *petC1* results in an increased expression of PetC2 (Fig. 2*A*). However, despite redox and functional similarities the PetC2-b_6f complex in this strain shows a significantly lower activity than could be expected on the basis of the amino acid sequence differences between PetC1 and PetC2 (Fig. 4*B*). The main reason for this is the small amount of functional cytochrome b_6f in this strain (as evidenced by immunoblot analysis, Fig. 2*A*), resulting in a constantly low electron transport rate (Fig. 4*B*).

The exact reason for this small PetC2-b_6f population size is unclear. However, because *petC1* and *petA* are organized in the *petCA* operon (58) it appears likely that *petC1* deletion also compromises expression of *petA* and thus accumulation of cytochrome *f*. Furthermore, the presence of PetC1 and/or cytochrome *f* appears to be critical for accumulation of SU IV but not for cytochrome b_6 (Fig. 2*A*). As these subunits are encoded by co-transcribed genes organized in the *petBD* operon (58) this reflects different stabilities of SU IV and cytochrome b_6 (59) in *Synechocystis* membranes. Although expression of *petC2* is clearly up-regulated upon deletion of *petC1* (Fig. 2*A*), this increased expression cannot fully compensate for PetC1 deficiency.

PetC2 and PetC3 Are Involved in Long-term Light Adaptation and Regulation of Cytochrome b_6f Complex Activity—Despite sequence differences between the two Rieske proteins, PetC2 can partially substitute PetC1 and mediate electron transfer from PQH_2 to cytochrome *f* (Fig. 4). However, due to its low abundance in WT thylakoid membranes (Fig. 2*A*) and the significant transcript accumulation under HL (Fig. 3), PetC2 is most likely mainly involved in regulatory processes. Furthermore, the Δ*petC2* strain has an unusually high growth rate under HL conditions in comparison to WT (Fig. 2*B*) suggesting a role of PetC2 in long-term light adaptation. As PetC1 and PetC2 are exclusively located in the thylakoid membrane (see below) and as the cytochrome b_6f complex only functions as a dimer, it would be interesting to know whether PetC1-b_6f and PetC2-b_6f form hybrid dimers or exclusively homodimers. Although important for understanding the molecular mechanism, the answer for this question is difficult and beyond the scope of this contribution.

PetC3 shows several unique features different from the other two Rieske isoforms in *Synechocystis*. First, the primary structure of PetC3 is quite different from PetC1 and PetC2 (38, 41). Its N-terminal region is shorter by more than 10 residues, the sequence of its putative transmembrane helix is poorly conserved, and the connected hinge region is lacking. All this might indicate a function of PetC3 that is different from the other two isoforms. In agreement with this, PetC3 was recently reported to be located exclusively in the cytoplasmic membrane of *Synechocystis* (55, 60). Also, as the Δ*petC1/2* double deletion strain does not survive (40), PetC3 apparently cannot functionally substitute PetC1, and the determined midpoint redox potential (+135 mV) is too negative to allow PetC3 to be a component of the linear electron transport chain (41). Although all these observations indicate that PetC3 is not a component of the "classical" cytochrome b_6f complex, our data show an impact on its function. A role of PetC3 in long-term light adaptation is supported by (*a*) the high growth rate of the Δ*petC3* mutant(s) under HL conditions (Fig. 2*B*) and (*b*) the observation that the maximal overall and linear electron transport rate is only achieved when all three PetC isoforms are present (Fig. 4*B*). The inability for an effective up-regulation of the cyclic electron transport relative to the linear one under HL in the Δ*petC3* strain (Fig. 4*C*) may also support this view. In summary, our data suggest defined roles of the various PetC proteins in short- and long-term light adaptation as a molecular basis for metabolic flexibility, which enables survival in an ever changing environment.

Acknowledgments—We are grateful for the excellent technical support of Ursula Altenfeld, Claudia König, Erdmut Thomas, and Dieter Wunsch, and for fruitful discussions with Jens Appel, Giovanni Finazzi, Yukako Hihara, Navassard Karapetyan, Teruo Ogawa, Thomas Pfannschmidt, and Alexander Ruban. We also acknowledge Friederike Koenig for providing access to spectroscopic equipment.

REFERENCES

1. Berry, S., Schneider, D., Vermaas, W. F., and Rögner, M. (2002) *Biochemistry* **41,** 3422–3429
2. Gutthann, F., Egert, M., Marques, A., and Appel, J. (2007) *Biochim. Biophys. Acta* **1767,** 161–169
3. Yeremenko, N., Jeanjean, R., Prommeenate, P., Krasikov, V., Nixon, P. J., Vermaas, W. F. J., Havaux, M., and Matthijs, H. C. P. (2005) *Plant Cell Phys.* **46,** 1433–1436
4. Allen, J. F. (2004) *Trends Plant Sci.* **9,** 130–137
5. Cape, J. L., Bowman, M. K., and Kramer, D. M. (2006) *Trends Plant Sci.* **11,** 46–55
6. Cramer, W. A., and Zhang, H. M. (2006) *Biochim. Biophys. Acta* **1757,** 339–345
7. Cramer, W. A., Zhang, H., Yan, J., Kurisu, G., and Smith, J. L. (2006) *Annu. Rev. Biochem.* **75,** 769–790
8. Cramer, W. A., Baniulis, D., Yamashita, E., Zhang, H., Zatsman, A. I., and Hendrich, M. P. (2008) in *Photosynthetic Protein Complexes, A Structural Approach* (Fromme, P., ed) pp. 155–179, Wiley-VCH, Weinheim
9. Bukhov, N., and Carpentier, R. (2004) *Photosynth. Res.* **82,** 17–33
10. Fork, D. C., and Herbert, S. K. (1993) *Photosynth. Res.* **36,** 149–168
11. Joliot, P., and Joliot, A. (2006) *Biochim. Biophys. Acta* **1757,** 362–368
12. Shikanai, T. (2007) *Annu. Rev. Plant Biol.* **58,** 199–217
13. Munekage, Y., Hashimoto, M., Miyake, C., Tomizawa, K., Endo, T., Tasaka, M., and Shikanai, T. (2004) *Nature* **429,** 579–582
14. Rumeau, D., Peltier, G., and Cournac, L. (2007) *Plant Cell Environ.* **30,** 1041–1051
15. Murata, N. (1969) *Biochim. Biophys. Acta* **172,** 242–251
16. Bonaventura, C., and Myers, J. (1969) *Biochim. Biophys. Acta* **189,** 366–383
17. Allen, J. F. (2003) *Science* **299,** 1530–1532
18. Wollman, F. A. (2001) *EMBO J.* **20,** 3623–3630
19. Finazzi, G., Rappaport, F., Furia, A., Fleischmann, M., Rochaix, J. D., Zito, F., and Forti, G. (2002) *EMBO Rep.* **3,** 280–285
20. Finazzi, G., and Forti, G. (2004) *Photosynth. Res.* **82,** 327–338
21. Vener, A. V., Van Kan, P. J., Gal, A., Andersson, B., and Ohad, I. (1995) *J. Biol. Chem.* **270,** 25225–25232
22. Vener, A. V., van Kan, P. J., Rich, P. R., Ohad, I., and Andersson, B. (1997) *Proc. Natl. Acad. Sci. U.S.A.* **94,** 1585–1590
23. Zito, F., Finazzi, G., Delosme, R., Nitschke, W., Picot, D., and Wollman, F. A. (1999) *EMBO J.* **18,** 2961–2969
24. Vener, A. V., Ohad, I., and Andersson, B. (1998) *Curr. Opin. Plant Biol.* **1,** 217–223
25. de Vitry, C., Ouyang, Y., Finazzi, G., Wollman, F. A., and Kallas, T. (2004) *J. Biol. Chem.* **279,** 44621–44627
26. Mullineaux, C. W., and Emlyn-Jones, D. (2005) *J. Exp. Bot.* **56,** 389–393
27. van Thor, J. J., Mullineaux, C. W., Matthijs, H. C. P., and Hellingwerf, K. J. (1998) *Bot. Acta* **111,** 430–443
28. Grossman, A. R., Schaefer, M. R., Chiang, G. G., and Collier, J. L. (1993) *Microbiol. Rev.* **57,** 725–749
29. MacColl, R. (1998) *J. Struct. Biol.* **124,** 311–334
30. Mullineaux, C. W. (2008) *Photosynth. Res.* **95,** 175–182
31. Mao, H. B., Li, G. F., Ruan, X., Wu, Q. Y., Gong, Y. D., Zhang, X. F., and Zhao, N. M. (2002) *FEBS Lett.* **519,** 82–86
32. Mullineaux, C. W., and Allen, J. F. (1986) *FEBS Lett.* **205,** 155–160
33. Whitelegge, J. P., Zhang, H., Aguilera, R., Taylor, R. M., and Cramer, W. A. (2002) *Mol. Cell Proteomics* **1,** 816–827
34. Schneider, D., Volkmer, T., and Rögner, M. (2007) *Res. Microbiol.* **158,** 45–50
35. Schneider, D., Berry, S., Rich, P., Seidler, A., and Rögner, M. (2001) *J. Biol. Chem.* **276,** 16780–16785
36. Zhang, H., Whitelegge, J. P., and Cramer, W. A. (2001) *J. Biol. Chem.* **276,** 38159–38165
37. Volkmer, T., Schneider, D., Bernát, G., Kirchhoff, H., Wenk, S. O., and Rögner, M. (2007) *J. Biol. Chem.* **282,** 3730–3737
38. Schneider, D., and Schmidt, C. L. (2005) *Biochim. Biophys. Acta* **1710,** 1–12
39. Kaneko, T., Sato, S., Kotani, H., Tanaka, A., Asamizu, E., Nakamura, Y., Miyajima, N., Hirosawa, M., Sugiura, M., Sasamoto, S., Kimura, T., Hosouchi, T., Matsuno, A., Muraki, A., Nakazaki, N., Naruo, K., Okumura, S., Shimpo, S., Takeuchi, C., Wada, T., Watanabe, A., Yamada, M., Yasuda, M., and Tabata, S. (1996) *DNA Res.* **3,** 109–136
40. Schneider, D., Berry, S., Volkmer, T., Seidler, A., and Rögner, M. (2004) *J. Biol. Chem.* **279,** 39383–39388
41. Schneider, D., Skrzypczak, S., Anemüller, S., Schmidt, C. L., Seidler, A., and Rögner, M. (2002) *J. Biol. Chem.* **277,** 10949–10954
42. Rippka, R., Deruelles, J., Waterbury, J. B., Herdman, M., and Stanier, R. Y. (1979) *J. Gen. Microbiol.* **111,** 1–61
43. Myers, J., Graham, J. R., and Wang, R. T. (1978) *J. Phycol.* **14,** 513–518
44. Bennett, A., and Bogorad, L. (1973) *J. Cell Biol.* **58,** 419–435
45. Bustin, S. A. (2002) *J. Mol. Endocrinol.* **29,** 23–39
46. Pfaffl, M. W. (2001) *Nucleic Acids Res.* **29,** e45
47. Ramakers, C., Ruijter, J. M., Deprez, R. H., and Moorman, A. F. (2003) *Neurosci. Lett.* **339,** 62–66
48. Pfaffl, M. W., Horgan, G. W., and Dempfle, L. (2002) *Nucleic Acids Res.* **30,** e36
49. Laemmli, U. K. (1970) *Nature* **227,** 680–685
50. Kovács, L., Damkjaer, J., Kereïche, S., Ilioaia, C., Ruban, A. V., Boekema, E. J., Jansson, S., and Horton, P. (2006) *Plant Cell* **18,** 3106–3120
51. Bernát, G., Waschewski, N., and Rögner, M. (2009) *Photosynth. Res.* **99,** 205–216
52. Alfonso, M., Perewoska, I., and Kirilovsky, D. (2000) *Plant Physiol.* **122,** 505–516
53. Howitt, C. A., and Vermaas, W. F. J. (1998) *Biochemistry* **37,** 17944–17951
54. Mogi, T., and Miyoshi, H. (2009) *J. Biochem.* **145,** 395–401
55. Schultze, M., Forberich, B., Rexroth, S., Dyczmons, N. G., Roegner, M., and Appel, J. (2009) *Biochim. Biophys. Acta*, in press
56. de Vitry, C., Finazzi, G., Baymann, F., and Kallas, T. (1999) *Plant Cell* **11,** 2031–2044
57. Yan, J., and Cramer, W. A. (2003) *J. Biol. Chem.* **278,** 20925–20933
58. Kallas, T., Spiller, S., and Malkin, R. (1988) *J. Biol. Chem.* **263,** 14334–14342
59. Kuras, R., and Wollman, F. A. (1994) *EMBO J.* **13,** 1019–1027
60. Aldridge, C., Spence, E., Kirkilionis, M. A., Frigerio, L., and Robinson, C. (2008) *Mol. Microbiol.* **70,** 140–150